Pergamon

Int. J. Heat Mass Transfer. Vol. 40, No. 7, pp. 1501–1508, 1997

0017-9310/97 $17.00+0.00

PII: S0017-9310(96)00257-8

Analysis of radiative heating of a rocket plume base with the finite-volume method

SEUNG WOOK BAEK and MAN YOUNG KIM

Department of Aerospace Engineering, Korea Advanced Institute of Science and Technology, 373-1 Kusong-Dong, Yusung-Gu, Taejon 305-701, Korea

(*Received* 18 *December* 1995 *and in final form* 2 *July* 1996)

Abstract—The finite-volume method for radiation is applied to investigate a radiative heating of rocket base plane due to searchlight and plume emissions. The exhaust plume is assumed to absorb, emit and scatter the radiant energy isotropically, as well as anisotropically, while the medium between the plume boundary and the base plane is cold and nonparticipating. The scattering phase function is modeled by a finite series of Legendre polynomials. After validating the benchmark solution by comparison with that of previous works obtained by the Monte-Carlo method, further investigations have been done by changing various parameters, such as plume cone angle, scattering albedo, scattering phase function, optical radius and nozzle exit temperature. The results show that the base plane is predominantly heated by the plume emission, rather than the searchlight emission, when the nozzle exit temperature is the same as that of plume. Copyright © 1996 Elsevier Science Ltd.

1. INTRODUCTION

The analysis of radiative base heating from rocket exhaust plumes has attracted considerable attention during the past few decades, since the base plane should be protected against radiative heating from rocket exhaust plumes. In addition, development of new propellants, which contain energetic binders and additives such as boron and aluminum, greatly increases the importance of radiative base heating [1]. Intrinsically the properties of gases and particles within exhaust plumes influence the thermal radiation process through absorbing, emitting and scattering characteristics. Therefore, models as well as methods for predicting rocket plume base heating, are in high demand.

Numerous practical engineering methods for calculation of the radiative base heating have been developed and widely used. While Tien and Abu-Romia [2] considered the rocket exhaust plume as a semi-infinite cylindrical absorbing and emitting gas body with uniform temperature and properties, Babco [3] and Edwards [4] treated it as a perfectly diffuse conical surface with axially varying radiosity. They used shape factor approximation from the exhaust plume to a different area such as the base plane. The thermal radiation from a cylindrical cloud of absorbing, emitting and anisotropically scattering particles has been investigated by Stockham and Love [5] using the Monte-Carlo method. It was found that the anisotropic scattering and searchlight emission play an important role in radiative base heating. Watson and Lee [6] employed the Monte-Carlo method to model the solid rocket booster plumes and considered axial and radial variations of the plume properties. The scattering was either isotropic or anisotropic therein. Recently, Nelson [7] adopted the backward Monte-Carlo method which is more computationally efficient than the direct Monte-Carlo method to predict radiative heating from conical isothermal, gray plumes. They also examined the effect of plume cone angle and searchlight emission.

Now that no single radiation model can solve all situations or all geometries encountered in engineering applications [8], engineers should select an appropriate method for their own specific concern. In order to predict the thermal radiation by a conical plume, its solution method must account for the grid skewness and the grid independency. In order to avoid these problems, the Monte-Carlo method has been used extensively to solve the problem of rocket plume base heating as observed before. However, this method has some inefficiencies and complexities in computation as well as incompatibility with other finite difference or volume methods. This fact drives us to find a more efficient method to evaluate the rocket plume base heating by thermal radiation such as the finite-volume method for radiation. This method was firstly derived by Chui and Raithby [9] and Chai *et al.* [10], and has been successfully applied to the problems of multidimensional cavity, of which geometries are complex or curvilinear. In this method, the total solid angle is divided into discrete number of directions and all directional intensities are calculated by the marching procedure as in the case for flux-type methods. Chui *et al.* [11] introduced the mapping that yields a complete solution by solving the intensity in a single azimuthal direction for the case of orthogonal

NOMENCLATURE

a^m coefficient of the general discretization equation, equations (5a)–(5c)
b^m source term in discretization equations, equation (5d)
D_{ci}^m directional weights, equation (4b)
$\mathbf{e}_x, \mathbf{e}_y, \mathbf{e}_z, \mathbf{e}_r$ unit vectors in x-, y-, z- and r-directions
G dimensionless radiation intensity
I actual radiation intensity
L characteristic length
M number of total radiation direction
$\mathbf{n}_i$ unit normal vector at i surface, $= n_{x,i}\mathbf{e}_x + n_{y,i}\mathbf{e}_y + n_{z,i}\mathbf{e}_z$, equation (4c)
$P_j(\cos\Psi)$ Legendre polynomial of order j
q_z^R radiative heat flux, equation (1)
R_{ex} radius of the nozzle exit, see Fig. 1
$\mathbf{r}$ position vector
S_r source term, equation (4d)
s distance traveled by a ray normalized by L
$\mathbf{s}$ unit direction vector
T temperature
x', y', z' directions parallel to the x-, y- and z-axes
Z_{pl} plume length, see Fig. 1.

Greek symbols
β_0 extinction coefficient, $= \kappa_a + \sigma_s$
$\Delta A_i, \Delta v$ surface area and volume of the control volume, respectively
$\Delta\Omega^m$ control angle, equation (4c)
ε_w wall emissivity
Θ dimensionless temperature, $= T/T_{ref}$
θ polar angle measured from the axial direction
κ_a absorption coefficient
σ Stefan-Boltzmann constant, $= 5.67 \times 10^{-8}$ [W m^{-2} K^{-4}]
σ_s scattering coefficient
τ_0 optical thickness
Φ scattering phase function
ϕ azimuthal angle measured from the radial direction, $= \varphi_\Omega - \varphi_0$
Ψ scattering angle between $\mathbf{s}'$ and $\mathbf{s}$
Ω solid angle
ω_0 scattering albedo
$\varphi_0, \varphi_\Omega$ space and angular variable in the azimuthal direction measured from x-axis, respectively, see Fig. 2.

Subscripts
E, W, N, S, T, B east, west, north, south, top and bottom neighbors of P
e, w, n, s, t, b east, west, north, south, top and bottom control volume faces
P nodal point in which intensities are located
$P+$, $P-$ boundaries of the control volume
w wall.

Superscripts
m, m' radiation direction
$m+$, $m-$ boundaries of the control angle.

axisymmetric radiation, and applied it to a general pulverized fuel flame to predict radiative heat transfer in furnace [12].

The main objective of this paper is to extend the orthogonal axisymmetric finite-volume method for radiation mentioned above to the non-orthogonal problem of thermal radiation model, i.e. the problem of rocket plume base heating. The plume is considered as an absorbing, emitting and isotropically or anisotropically scattering medium, while the medium between plume boundary and rocket base plane is nonparticipating. The scattering phase function is modeled by a finite series of Legendre polynomials [13]. After validating our solutions by comparison with those of previous works, detailed investigation of the radiative base heating due to searchlight emission and plume emission is conducted by changing various parameters such as plume cone angle, scattering albedo, scattering phase function, optical radius and nozzle exit temperature.

2. ANALYSIS

2.1. *Model description*

Schematic of the radiative base heating due to searchlight emission and plume emission is shown in Fig. 1. δ, R_{ex} and Z_{pl} are the plume cone angle, radius of nozzle exit and plume length, respectively. The exhaust plume emerged from the nozzle exit at $z = 0$ has a cylindrical shape when $\delta = 0°$ and a finite conical shape when $\delta \neq 0°$. Searchlight emission is caused by photons which are emitted from the inside of rocket nozzle and then scattered by the exhaust plume toward the base plane. On the other hand, the plume emission is due to photons emitted directly from the exhaust plume.

Exhaust plume is treated as radiatively participating medium, which is surrounded by a cold and nonparticipating medium. No other external incidence of radiant energy is considered here and the plume boundary is considered free. Instead of using shape

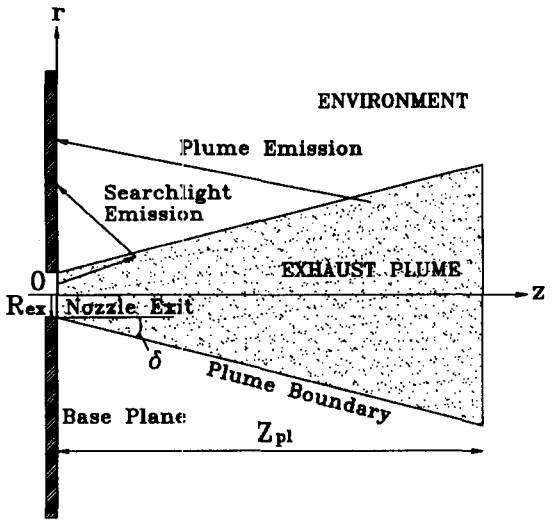

Fig. 1. Schematic of the rocket plume base heating.

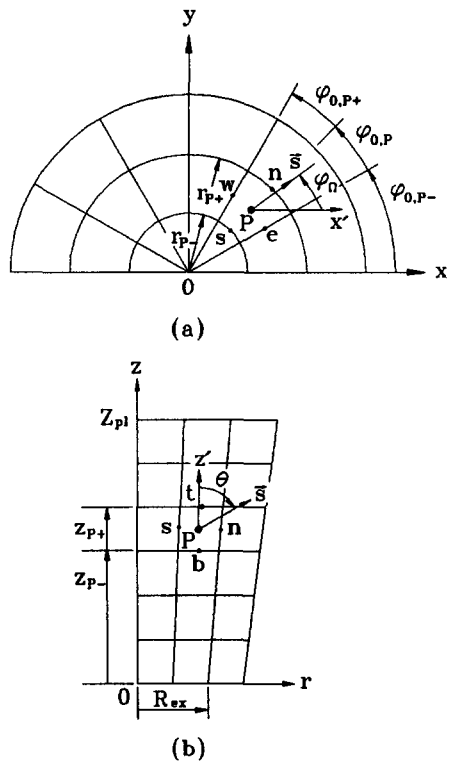

Fig. 2. Top and side views of spatial control volume and typical radiation direction: (a) top view; (b) side view.

factor approximation, the finite-volume method for radiation is adopted here, covering full domain including exhaust plume and environment. For simplicity, the exhaust plume is assumed to have uniform temperature and constant properties, not dependent on space and wavelength.

2.2. *Radiative transfer equation*

In order to compute the radiative heat flux at base plane, the radiative transfer equation, which is an energy balance for radiation intensity, must be solved, since the radiative heat flux, q_z^R at base plane is defined as

$$q_z^R = \int_{\Omega=4\pi} I(\mathbf{r}_w, \mathbf{s})(\mathbf{s}\cdot\mathbf{n}_w)\,d\Omega \tag{1}$$

where, $I(\mathbf{r}_w, \mathbf{s})$ is the radiation intensity at position $\mathbf{r}_w$ and direction $\mathbf{s}$, $\mathbf{n}_w$ is the unit normal vector at the base plane, and Ω is the solid angle. For a gray medium, the radiation intensity at any position, $\mathbf{r}$, along a path, $\mathbf{s}$ through an absorbing, emitting and scattering medium can be given by [14]

$$\frac{1}{\tau_0}\frac{dG(\mathbf{r},\mathbf{s})}{ds} = -G(\mathbf{r},\mathbf{s}) + (1-\omega_0)\Theta^4(\mathbf{r}) + \frac{\omega_0}{4\pi}\int_{\Omega=4\pi} G(\mathbf{r},\mathbf{s}')\Phi(\mathbf{s}',\mathbf{s})\,d\Omega' \tag{2}$$

where, $G(\mathbf{r},\mathbf{s}) = \pi I(\mathbf{r},\mathbf{s})/\sigma T_{ref}^4$ is the dimensionless radiation intensity, $\tau_0 = \beta_0 L$ is the optical thickness, $\omega_0 = \sigma_s/\beta_0$ is the scattering albedo and $\Phi(\mathbf{s}',\mathbf{s})$ is the scattering phase function of energy transfer from the incoming direction $\mathbf{s}'$ to the scattered direction $\mathbf{s}$. In cylindrical coordinates, $G(\mathbf{r},\mathbf{s})$ actually represents $G(r,\varphi_0,z,\theta,\phi)$ where $\phi = \varphi_\Omega - \varphi_0$ is the azimuthal angle. This equation, if the temperature of the medium, $\Theta(\mathbf{r})$ and the boundary conditions for intensity are given, produces local radiation intensity. For a diffusely emitting and reflecting wall with temperature Θ_w, the outgoing intensity at the wall can be expressed as the summation of emitted and reflected ones

$$G(\mathbf{r}_w,\mathbf{s}) = \varepsilon_w\Theta^4(\mathbf{r}_w) + \frac{1-\varepsilon_w}{\pi}\int_{\mathbf{s}\cdot\mathbf{n}_w<0} G(\mathbf{r}_w,\mathbf{s}')|\mathbf{s}'\cdot\mathbf{n}_w|\,d\Omega' \tag{3}$$

where, ε_w is the wall emissivity and subscript w denotes the wall location, while $\mathbf{n}$ is the unit normal vector.

2.3. *The finite-volume method for radiation*

In order to derive the discretization equation, the equation (2) is integrated over a control volume, Δv, and a control angle, $\Delta\Omega^m$, as shown in Figs. 2 and 3. It was assumed that the magnitude of intensity is constant over a given control volume and a control angle, but its direction may vary. After integration, the following finite-volume formulation can be obtained:

$$\sum_{i=e,w,n,s,t,b} G_i^m\,\Delta A_i D_{ci}^m = \tau_0(-G^m + S_r^m)_p\Delta v\Delta\Omega^m \tag{4a}$$

where

$$D_{ci}^m = \int_{\Delta\Omega^m}(\mathbf{s}\cdot\mathbf{n}_i)\,d\Omega^m \tag{4b}$$

$$\mathbf{n}_i = \mathbf{n}_{x,i}\mathbf{e}_x + n_{y,i}\mathbf{e}_y + n_{z,i}\mathbf{e}_z \tag{4c}$$

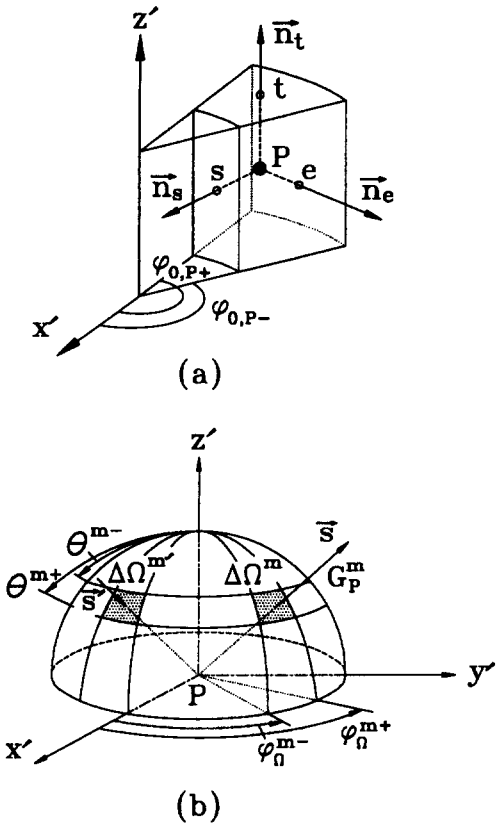

Fig. 3. Infinitesimal spatial control volume and control angle: (a) infinitesimal spatial control volume; (b) angular discretization.

$$S_r^m = (1-\omega_0)\Theta^4 + \frac{\omega_0}{4\pi}\int_{\Omega'=4\pi} G_P^{m'}\,\Phi^{m'm}\,\mathrm{d}\Omega' \quad (4d)$$

$$\Delta\Omega^m = \int_{m-}^{m+}\mathrm{d}\Omega^m = \int_{\varphi_\Omega^{m-}}^{\varphi_\Omega^{m+}}\int_{\theta^{m-}}^{\theta^{m+}}\sin\theta\,\mathrm{d}\theta\,\mathrm{d}\varphi_\Omega \quad (4e)$$

and ΔA_i and Δv represent the surface area and control volume, respectively, while $\mathbf{n}_i$ is the outward unit normal vector at control volume face and $G^m = G(\mathbf{r}, \mathbf{s})$. This equation indicates that the net outgoing radiant energy out of the control volume must be balanced by net generation of radiant energy within control volume and control angle. Therefore, the directional weight, D_{ci}^m [15] should be carefully evaluated since it represents inflow or outflow of radiant energy across that control volume face depending on its sign.

There have been many schemes which relate control volume face intensity to the nodal intensity. Although the diamond scheme, the positive scheme by Fieland [16], variable weight scheme by Jamaluddin and Smith [17], Kim *et al.* [18] and Baek *et al.* [19], and the exponential-type scheme by Carlson and Lathrop [20], Chui *et al.* [9, 11, 12] and Chai *et al.* [10] are available, the step scheme is chosen here. This scheme sets the downstream face intensity to be equal to the upstream nodal intensity [10]. Although this simple and convenient scheme ensures positive intensity, while not considering geometric and directional complexities, it may degenerate the solution accuracy. In this method, the radiation cannot be directly transferred to adjacent element contacting at each corner of the control volume of interest so that inherently, a certain amount of errors could exist. By making use of the step scheme, the above equation can be recast into the following general discretization equation for an arbitrary radiation direction

$$a_P^m G_P^m = a_E^m G_E^m + a_W^m G_W^m + a_N^m G_N^m + a_S^m G_S^m + a_T^m G_T^m + a_B^m G_B^m + b_P^m \quad (5a)$$

where

$$a_I^m = \max[-\Delta A_i D_{ci}^m, 0] \quad (5b)$$

$$a_P^m = \sum_{i=\mathrm{e,w,n,s,t,b}} \max[\Delta A_i D_{ci}^m, 0] + \tau_{0,P}\Delta v\Delta\Omega^m \quad (5c)$$

$$b_P^m = (\tau_0 S_r^m)_P \Delta v \Delta\Omega^m. \quad (5d)$$

In equation (5b), the subscript I represents E, W, N, S, T and B, while i stands for e, w, n, s, t and b, respectively.

Control volume and control angle used in this work are plotted in Figs. 2 and 3. The total number of the control volume discretized is $(N_r \times N_{\varphi_0} \times N_z)$. Each control volume is composed of a series of planes at right angles to the plume axis, i.e. top and bottom surfaces, and surface emanating from a same vertex like that of Watson and Lee [6], which is different from that of Chui *et al.* [11]. Therefore, ΔA_i and Δv should be calculated carefully according to grid skewness. The control angle is designed in the same way as a typical solid angle. The total solid angle, 4π is divided into $(N_\theta \times N_{\varphi_\Omega}) = M$ directions, where θ is the polar angle and φ_Ω is the azimuthal angle, ranging from 0 to π and from 0 to 2π, respectively. A calculation procedure is completed when the following constraint is met;

$$\max[|G_P^m - G_P^{m,\mathrm{old}}|/G_P^m] \leqslant 10^{-6} \quad (6)$$

where $G_P^{m,\mathrm{old}}$ is the previous iteration value of G_P^m.

2.4. *Solution procedure*

To solve asymmetric radiation problems in cylindrical enclosure, the directional intensity $G^m = G(r, \varphi_0, z, \theta, \varphi_\Omega)$ must be obtained from equation (5) in each direction m and at each nodal point. The solution procedure for the finite-volume method is iterative in the same way as the discrete ordinates method [18]. The calculation is started from the boundary where the outgoing intensity is given as boundary condition and then proceeds into the inner nodes. A marching principle is quite straightforward, i.e. at one azimuthal location, it radially marches from outside toward center when $D_{cn}^m < 0$ or vice versa, and from bottom to top along the axial direction when $D_{ct}^m > 0$ or vice versa.

If the radiation field is axisymmetric, Chui *et al.*

[11] showed that it is sufficient to solve for intensity $G(r, \varphi_0, z, \theta, \varphi_\Omega = 0)$ through the mapping that transforms the axisymmetric intensity $G(r, z, \theta, \phi)$ to $G(r, \varphi_0, z, \theta, \varphi_\Omega = 0)$ if $\Delta\varphi_0 = \Delta\varphi_\Omega$ is satisfied. In other words, the dependence of intensity on two-space and two-angle can be converted into on three-space and one-angle so that the general discretization equation developed in the three-dimensional case can be used without loss of generality. In this work, the intensity is symmetric about $y = 0$ so that it is calculated only on the domain of $y \geqslant 0$. The marching procedure for symmetric case becomes the same as for the asymmetric case except that φ_Ω sweep is not necessary in axisymmetric radiation. It must also be noted that a difficulty in calculating angular derivatives, that is encountered in discrete-ordinates method because of the lack of conservation and unphysical directional coupling [11, 20], does not arise in the finite-volume method used here.

2.5. *Boundary conditions*

For a diffusely emitting and reflecting wall with Θ_w, the outgoing intensity in equation (3) can be discretized as

$$G_w^m = \varepsilon_w \Theta_w^4 + \frac{1-\varepsilon_w}{\pi} \sum_{D_{cw}^{m'}<0} G_w^{m'} |D_{cw}^{m'}|. \qquad (7)$$

However, the intensity at base plane is $G_w^m = 0$, since it is assumed to be cold and black. The intensities along the symmetry plane, $y = 0$ are trivial, because corresponding coefficients in the discretized equation (5) are zero, which derives from the fact that $\Delta A_i = 0$ along the z-axis and $D_{ci}^m = 0$ along the $y = 0$ plane except for the z-axis.

3. RESULTS AND DISCUSSIONS

3.1. *Comparison to previous works*

Previous exhaust plume studies by the Monte-Carlo method [5] and the backward Monte-Carlo method [7] have been chosen to validate present numerical solutions obtained by the finite-volume method for radiation. Nozzle exit radius R_{ex} is chosen as a characteristic length of the exhaust plume. The corresponding optical radius is $\tau_0 = 0.5$ and plume length is $Z_{pl} = 10R_{ex}$. The exhaust plume is assumed to be cold ($T = 0$) and purely scatters ($\omega_0 = 1$) the radiant energy that is isotropically emerged from the nozzle exit with the temperature T_{ref}. The environment is considered cold and nonparticipating. This situation represents a so-called searchlight emission as shown in Fig. 1 because the radiation is only emitted from the rocket nozzle exit.

Current results for the nondimensional radiative heat flux, $q_z^R/\sigma T_{ref}^4$ are plotted as a function of r/R_{ex} at the base plane and compared with other results in Fig. 4. As r/R_{ex} increases, the base plane views a smaller portion of the exhaust plume. Therefore, the radiative heat flux emerging from the nozzle exit rapidly decreases as r/R_{ex} increases. As shown in the figure, the agreement between the finite-volume method and the Monte-Carlo method is quite good. In this work, a computational domain is taken as $z/R_{ex} = 10$ long and $r/R_{ex} = 6$ wide. Two angular grid systems, $(N_{\varphi_0} \times N_\theta) = (6 \times 4)$ or (10×8), are used while the spatial grid system is $(N_r \times N_z) = (40 \times 50)$. It takes about 10 min on a 486 DX2-66 MHz IBM PC, when $(N_{\varphi_0} \times N_\theta) = (6 \times 4)$ (which is analogous to the S_4 discrete-ordinates method [18] in the number of radiation directions used). For the case of $(N_{\varphi_0} \times N_\theta) = (10 \times 8)$ corresponding to S_8 discrete-ordinates method, the results become more accurate. However, the computational time increases to as much as about 70 min on the same computer.

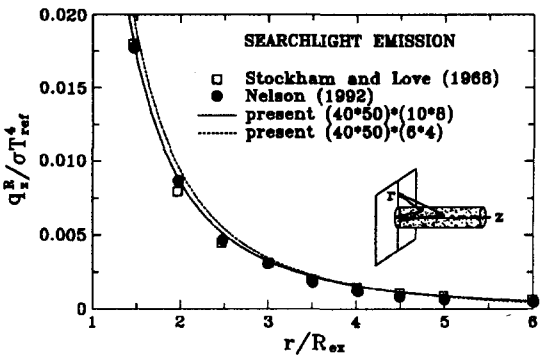

Fig. 4. Base heating due to searchlight emission for the case of $\delta = 0°$. Cylindrical exhaust plume with $Z_{pl}/R_{ex} = 10$ has $\omega_0 = 1$ and $\tau_0 = 0.5$. Scattering is isotropic.

3.2. *Rocket plume base heating*

In order to illustrate the applicability of the finite-volume method used here, results obtained by parametric study will be presented in the following. The parameters chosen include the plume cone angle, δ, scattering albedo, ω_0, forward, isotropic and backward scattering phase functions, optical radius, τ_0 and nozzle exit temperature. For all the cases discussed below, the plume length is $Z_{pl}/R_{ex} = 50$ and spatial grid system is $(N_r \times N_z) = (40 \times 70)$. The angular grid system is $(N_{\varphi_0} \times N_\theta) = (6 \times 4)$ for $\delta = 0°$ and $(N_{\varphi_0} \times N_\theta) = (8 \times 6)$ for $\delta = 15°$.

Figure 5 shows the effect of scattering albedo on the base heating due to searchlight and plume emissions for $\tau_0 = 0.5$ with isotropic scattering. It must be noticed that the temperature of exhaust plume is the same as the nozzle exit temperature, i.e. uniform temperature, T_{ref}. As the scattering albedo ω_0 increases, the heat flux at the base plane is significantly reduced since the plume emission decreases. For the case of $\omega_0 = 0$ the searchlight emission becomes negligible so that two curves become overlapped. However, as the scattering albedo increases, the searchlight emission is seen to increase, which can be deduced by subtracting

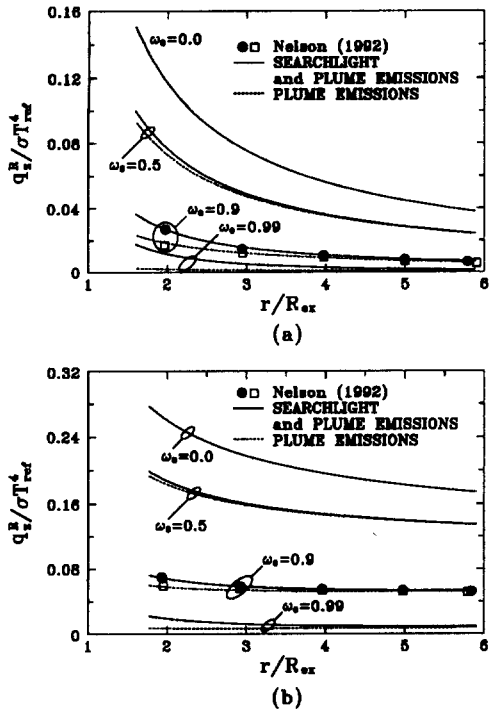

Fig. 5. Effect of scattering albedo on the base heating due to searchlight emission and/or plume emission. Exhaust plume with $Z_{pl}/R_{ex} = 50$ has $\tau_0 = 0.5$. Scattering is isotropic: (a) $\delta = 0°$; (b) $\delta = 15°$.

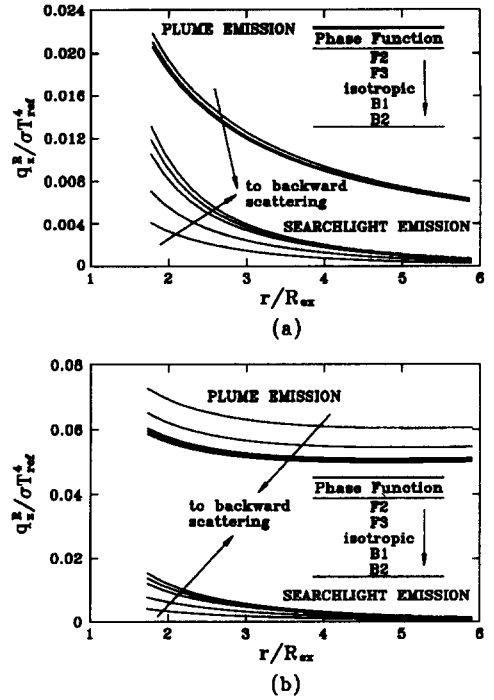

Fig. 6. Effect of scattering phase function on the base heating due to searchlight emission or plume emission. Exhaust plume with $Z_{pl}/R_{ex} = 50$ has $\omega_0 = 0.9$ and $\tau_0 = 0.5$: (a) $\delta = 0°$; (b) $\delta = 15°$.

the dotted line from the solid line. It is also apparent that base heating increases as the cone angle increases. For the case of $\omega_0 = 1$, the radiative base heating entirely occurs by searchlight emission for there is no emission by the exhaust plume. When the plume cone angle is changed from 0 to 15°, the amount of radiative heating basically increases. However, the ratio of searchlight emission to plume emission decreases for the same scattering albedo. In other words the plume emission starts to play a more significant role. Comparison of the current results with Nelson's results by backward Monte-Carlo method [7] for the case of $\omega_0 = 0.9$ shows a good agreement for both $\delta = 0°$ and $\delta = 15°$.

In the above, the scattering is already shown to exert a strong influence on the base heating. It is, then, desirable to study the effect of anisotropic scattering. In this study the scattering phase function is approximated by a finite series of Legendre polynomials as follows

$$\Phi(\mathbf{s}', \mathbf{s}) = \Phi(\cos\Psi) = \sum_{j=0}^{J} C_j P_j(\cos\Psi) \qquad (8)$$

where Ψ is the scattering angle between incident direction, $\mathbf{s}'$, and scattered direction, $\mathbf{s}$. C_j are the expansion coefficients that depend on the size and refractive index of the scattering particle. The forward ($F2, F3$) and backward ($B1, B2$) scattering phase function as given by Kim and Lee [13] are considered in addition to isotropic scattering. The asymmetry factors in the phase function for cases of $F2$, $F3$, isotropic, $B1$ and $B2$ are 0.670, 0.40, 0.0, −0.188 and −0.40, respectively. In Fig. 6 their effects on the radiative base heating are presented for $\omega_0 = 0.9$ and $\tau_0 = 0.5$. Depending on the emission type, i.e. plume or searchlight emission, the effect of scattering type on the base heating is found to be different as shown in the figure. While the forward scattering enhances the radiative energy transfer from the plume towards the base plane for the case of plume emission, the backward scattering causes an increase in the radiative heat flux on the base plane for the case of searchlight emission. When the plume cone angle is increased to 15°, the radiative heat flux at the base plane becomes more uniform, which is quite obvious, considering the geometric sense.

The effect of optical radius on the base heating due to searchlight and plume emissions for the isotropic scattering phase function with $\omega_0 = 0.9$ is plotted in Fig. 7. Five different optical radii have been chosen. Since the optical radius represents a ratio of characteristic length of the system to mean penetration length of the radiation, with increasing the optical radius more radiation can be absorbed and emitted by the exhaust plume. Therefore, more radiative energy can be transferred from the plume to the base plane as the optical radius increases. It must be also noted that a ratio of searchlight emission to the plume emission initially increases and then decreases as the optical radius increases. When the plume cone angle is changed from 0 to 15°, the radiative heat flux at the

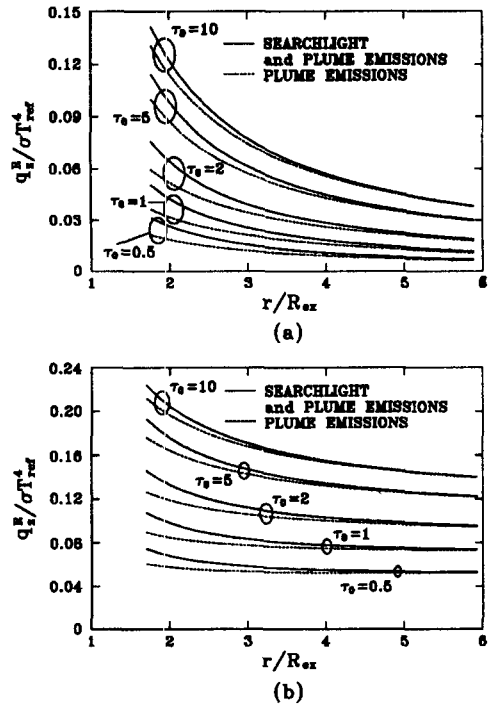

Fig. 7. Effect of optical radius on the base heating due to searchlight emission and/or plume emission. Exhaust plume with $Z_{pl}/R_{ex} = 50$ has $\omega_0 = 0.9$. Scattering is isotropic: (a) $\delta = 0°$; (b) $\delta = 15°$.

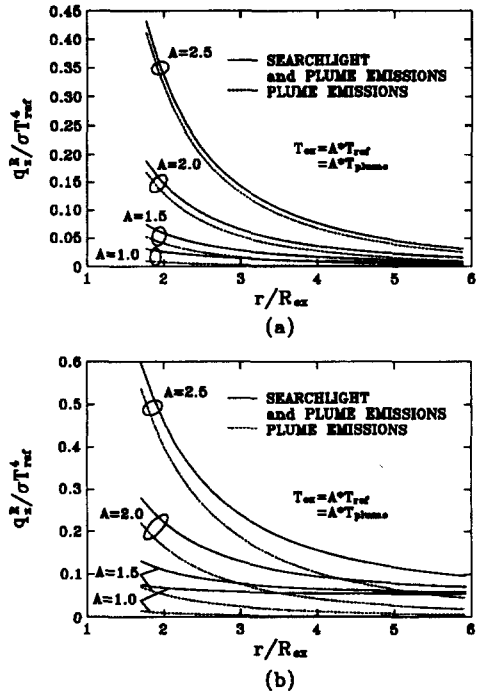

Fig. 8. Effect of nozzle exit temperature on the base heating due to searchlight emission and/or plume emission. Exhaust plume with $Z_{pl}/R_{ex} = 50$ has $\omega_0 = 0.9$ and $\tau_0 = 0.5$. Scattering is isotropic: (a) $\delta = 0°$; (b) $\delta = 15°$.

base plane increases at the same optical radius, which is evident from geometric reason.

As seen from the above discussion, when plume temperature and nozzle exit temperature are at the same uniform temperature, T_{ref}, the effect of searchlight emission on base heating is usually less than that of plume emission. Figure 8 shows the effect of nozzle exit temperature on the base heating for $\omega_0 = 0.9$ and $\tau_0 = 0.5$. The nozzle exit temperature is varied from 1 to 1.5, 2 and 2.5 times plume temperature, T_{ref}. As the nozzle exit temperature increases, the searchlight emission significantly increases such that the base heating by searchlight emission already exceeds that by plume emission when the nozzle exit temperature becomes 1.5 times plume temperature for the case of $\delta = 0°$. When the nozzle exit temperature is twice as much as the exhaust plume temperature, the radiative heat flux at base plane by searchlight emission increases by a factor of 16. The radiative base heating by searchlight emission is seen to increase with increasing plume cone angle.

4. CONCLUSIONS

The finite-volume method for radiation has been used to analyse the rocket plume base heating. The exhaust plume is considered to absorb, emit and scatter radiant energy isotropically as well as anisotropically, but the medium in the environment is not participating. The effects of plume cone angle, scattering albedo, scattering phase function, optical radius and nozzle exit temperature are examined in view of plume and searchlight emissions. The main results show that:

(1) the rocket base is predominantly heated by the plume emission compared with the searchlight emission, when the nozzle exit temperature is the same as the plume temperature;

(2) as the plume cone angle increases from 0 to 15°, radiative heat flux on the base plane increases;

(3) as the scattering albedo increases, the plume emission decreases, whereas the searchlight emission increases;

(4) while the forward scattering enhances the base heating for the case of plume emission, the backward scattering does for the case of searchlight emission;

(5) as the optical radius increases, the radiative base heating by plume emission increases, but the searchlight emission initially increases and then decreases;

(6) as the nozzle exit temperature increases with plume temperature fixed, the role by searchlight emission starts to exceed that of plume emission in the radiative base heating.

Acknowledgement—The financial assistance by the Objective Research Fund of the Korea Science and Engineering Foundation is gratefully acknowledged.

REFERENCES

1. Reardon, J. E. and Nelson, H. F., Rocket plume base heating methodology. *Journal of Thermophysics & Heat Transfer*, 1994, **8**, 216–222.

2. Tien, C. L. and Abu-Romia, M. M., A method of calculating rocket plume radiation to the base region. *Journal of Spacecraft & Rockets*, 1964, **1,** 433–435.
3. Babco, R. P., Radiation from conical surfaces with nonuniform radiosity. *AIAA Journal*, 1966, **4,** 544–546.
4. Edwards, D. K., Comment on radiation from conical surfaces with nonuniform radiosity. *AIAA Journal*, 1969, **7,** 1656–1658.
5. Stockham, L. W. and Love, T. J., Radiative heat transfer from a cylindrical cloud of particles. *AIAA Journal*, 1968, **6,** 1935–1940.
6. Watson, G. H. and Lee, A. L., Thermal radiation model for solid rocket booster plumes. *Journal of Spacecraft and Rockets*, 1977, **14,** 641–647.
7. Nelson, H. F., Backward Monte Carlo modeling for rocket plume base heating. *Journal of Thermophysics & Heat Transfer*, 1992, **6,** 556–558.
8. Howell, J. R., Thermal radiation in participating media : the past, the present, and some possible futures. *Journal of Heat Transfer*, 1988, **110,** 1220–1226.
9. Chui, E. H. and Raithby, G. D., Computation of radiant heat transfer on a nonorthogonal mesh using the finite-volume method. *Numerical Heat Transfer, Part B*, 1993, **23,** 269–288.
10. Chai, J. C., Lee, H. S. and Patankar, S. V., Finite-volume method for radiation heat transfer. *Journal of Thermophysics & Heat Transfer*, 1994, **8,** 419–425.
11. Chui, E. H., Raithby, G. D. and Hughes, P. M. J., Prediction of radiative transfer in cylindrical enclosures with the finite-volume method. *Journal of Thermophysics & Heat Transfer*, 1992, **6,** 605–611.
12. Chui, E. H., Hughes, P. M. J. and Raithby, G. D., Implementation of the finite-volume method for calculating radiative transfer in a pulverized fuel flame. *Combustion Science & Technology*, 1993, **92,** 225–242.
13. Kim, T. K. and Lee, H. S., Radiative heat transfer in two-dimensional anisotropic scattering media with collimated incidence. *Journal of Quantitative Spectroscopy & Radiation Transfer*, 1989, **42,** 225–238.
14. Ozisik, M. N., *Radiative Transfer and Interactions with Conduction and Convection*. Wiley, New York, 1973.
15. Kim, M. Y. and Baek, S. W., Numerical analysis of conduction, convection and radiation in a gradually expanding channel. *Numerical Heat Transfer, Part A*, 1996, **29,** 725–740.
16. Fiveland, W. A., A discrete-ordinates method for predicting radiative heat transfer in axisymmetric enclosure. ASME Paper 82-HT-20, 1982.
17. Jamaluddin, A. S. and Smith, P. J., Predicting radiative transfer in axisymmetric cylindrical enclosures using the discrete-ordinates method. *Combustion Science & Technology*, 1988, **62,** 173–186.
18. Kim, J. S., Baek, S. W. and Kaplan, C. R., Effect of radiation on diffusion flame behavior over a combustible solid. *Combustion Science Technology*, 1992, **88,** 133–150.
19. Baek, S. W., Kim, T. Y. and Lee, J. S., Transient cooling of a finite cylindrical medium in the rarefied cold environment. *International Journal of Heat and Mass Transfer*, 1993, **36,** 3949–3956.
20. Carlson, B. G. and Lathrop, K. D., Transport theory—the method of discrete ordinates. In *Computing Methods in Reactor Physics*, ed. H. Greenspan, C. N. Kelber and D. Okren. Gordon and Breach, New York, 1968, pp. 165–266.